Identification of a CDH12 potential candidate genetic variant for an autosomal dominant form of transgrediens and progrediens palmoplantar keratoderma in a Tunisian family

Cherine Charfeddine, Hamza Dallali, Ghaith Abdessalem, Kais Ghedira, Yosr Hamdi, Sahar Elouej, Zied Landoulsi, Valérie Delague, Arnaud Lagarde, Nicolas Levy, et al.

Journal of Human Genetics (2020) 65:397–410
https://doi.org/10.1038/s10038-019-0711-4

ARTICLE

Identification of a *CDH12* potential candidate genetic variant for an autosomal dominant form of transgrediens and progrediens palmoplantar keratoderma in a Tunisian family

Cherine Charfeddine[1,2] · Hamza Dallali[1] · Ghaith Abdessalem[1] · Kais Ghedira[3] · Yosr Hamdi[1] · Sahar Elouej[1,8] · Zied Landoulsi[1,4] · Valérie Delague[8] · Arnaud Lagarde[8] · Nicolas Levy[8] · Aziz El-Amraoui[5] · Mohamed Samir Boubaker[6] · Sonia Abdelhak[1] · Mourad Mokni[7]

Received: 22 March 2019 / Revised: 29 November 2019 / Accepted: 1 December 2019 / Published online: 7 January 2020

Abstract

Molecular diagnosis of rare inherited palmoplantar keratoderma (PPK) is still challenging. We investigated at the clinical and genetic level a consanguineous Tunisian family presenting an autosomal dominant atypical form of transgrediens and progrediens PPK to better characterize this ultrarare disease and to identify its molecular etiology. Whole-exome sequencing (WES), filtering strategies, and bioinformatics analysis have been achieved. Clinical investigation and follow up over 13 years of this Tunisian family with three siblings formerly diagnosed as an autosomal recessive form of Mal de Melela-like conducted us to reconsider its initial phenotype. Indeed, the three patients presented clinical features that overlap both Mal de Meleda and progressive symmetric erythrokeratoderma (PSEK). The mode of inheritance was also reconsidered, since the mother, initially classified as unaffected, exhibited a similar expression of the disease. WES analysis showed the absence of potentially functional rare variants in known PPKs or PSEK-related genes. Results revealed a novel heterozygous nonsynonymous variant in cadherin-12 gene (*CDH12*, NM_004061, c.1655C > A, p.Thr552Asn) in all affected family members. This variant is absent in dbSNP and in 50 in-house control exomes. In addition, in silico analysis of the mutated 3D domain structure predicted that this variant would result in cadherin-12 protein destabilization and thermal instability. Functional annotation and biological network construction data provide further supporting evidence for the potential role of *CDH12* in the maintenance of skin integrity. Taken together, these results suggest that *CDH12* gene is a potential candidate gene for an atypical presentation of an autosomal dominant form of transgrediens and progrediens PPK.

Introduction

Inherited disorders of cornification span a wide clinical spectrum. The broad clinical overlap between different groups, such as ichthyoses, erythrokeratodermas, and palmoplantar keratoderma (PPK), as well as the inter- and intrafamilial variability of many disorders make their distinction particularly challenging. Moreover, the unfamiliarity

✉ Cherine Charfeddine
cherine.charfeddine@gmail.com

1 Laboratory of Biomedical Genomics and Oncogenetics, LR16IPT05, Pasteur Institute of Tunis, University of Tunis El Manar, Tunis, Tunisia

2 High Institute of Biotechnology of Sidi Thabet, Biotechpole of Sidi Thabet, University of Manouba, 2020 Ariana, Tunisia

3 Laboratory of Bioinformatics, Biomathematics and Biostatistics - LR16IPT09, Pasteur Institute of Tunis, University Tunis El Manar, Tunis, Tunisia

4 Bioinformatics Core, Luxembourg Centre for Systems Biomedicine, University of Luxembourg, Esch-Sur-Alzette, Luxembourg

5 Génétique et Physiologie de l'Audition, Institut Pasteur, INSERM UMRS1120, Sorbonne University, 75015 Paris, France

6 Laboratory of Human and Experimental Pathology, Pasteur Institute of Tunis, Tunis, Tunisia

7 Department of Dermatology, CHU La Rabta Tunis, 1007 Tunis, Tunisia

8 Present address: Marseille Medical Genetics U 1251, Aix Marseille Université Faculté de Médecine de la Timone, Marseille, France

of physicians with some extremely rare phenotypes, coupled with clinical and genetic heterogeneity, often makes it very difficult to establish accurate diagnosis. Over the past 20 years, substantial progress has been made in discovering the genetic bases of inherited skin disorders. For most of these disorders, the discovery of underlying gene defects has relied on assembling large pedigrees or a number of similarly affected individuals or families and then applying molecular genetic methods of genome-wide linkage, homozygosity mapping, and gene sequencing [1, 2]. The advent of next-generation sequencing however opens new opportunities for combining clinical to molecular diagnosis, which would enable discovery of disease causal variants and a better definition and characterization of the still unknown molecular and cellular mechanisms involved in many forms of inherited genodermatoses [3, 4].

Our study group, among others, has a longstanding interest in understanding the molecular etiology of rare genodermatoses in addition to unraveling uncommon clinical features of these diseases [5, 6].

We report here on a large consanguineous Tunisian family (MDM-JL) including three siblings diagnosed as an autosomal recessive form of Mal de Meleda (MDM)-like for which molecular etiology is unknown. Long term follow up of this family revealed that the mother had similar manifestations to those observed in her affected offsprings. This prompted us to reconsider the initial clinical diagnosis and the inheritance mode of this atypical PPK, followed by a genotypic analysis that revealed the involvement of a new potential candidate pathogenic variant.

Materials and methods

Patients

This study was conducted according to the principles of the declaration of Helsinki and to the ethical standards of the authors Institutional Review Board (registration number IRB00005445, FWA00010074).

Written informed consent was obtained from all patients before their participation in the study. The family pedigree described here was previously documented in a published genetic study [7] but has recently been updated. Three affected siblings, their affected mother, and unaffected brother were included in this study.

Whole-exome sequencing (WES) and bioinformatic analysis

WES was performed for two affected cases (MDM-JL-V-2 and JL-V-8), the affected mother (JL-IV-6), and unaffected sib (JL-V-4) (Fig. 1a).

Exome was captured from genomic DNA using Agilent SureSelect Human All Exon V5 kit for the three patients and Agilent SureSelect Clinical Research Exome kit for the unaffected member. Libraries were sequenced on an Illumina HiSeq 2000 sequencer using 100-bp paired-end reads. Sequence reads were aligned against the GRGh37 (hg19) human reference assembly, yielding Binary Alignment/Map files, from which SNPs and short indels were called for each individual sample and reported in variant call format. Variants were filtered to include only those with >20× read depth and mapping quality score >=30. Functional annotation of variants was carried out using VarAft software version 2.06 (http://varaft.eu/index.php).

All variants then underwent a mixed filtering/prioritization strategy to reach a small number of potential candidate variants. First, variants found in coding sequences, splicing, upstream, downstream, and 5′-and 3′ UTRs were considered for the analysis. Variants were retrieved when being missense, nonsense, frameshift, in-frame indels, and affecting splicing. The next step was to remove variants with minor allele frequency (MAF) >0.01 in the dbSNP, Exome Aggregation Consortium database (ExAC), Cambridge, MA (http://exac.broadinstitute.org) and 1000 Genomes (http://www.internationalgenome.org). Finally, the pathogenicity of the remaining non-synonymous genetic variants was assessed in silico by six prediction algorithms: MutationTaster (http://www.mutationtaster.org/; PolyPhen (http://genetics.bwh.harvard.edu/pph2/), combined annotation dependent depletion (CADD > 15) (http://cadd.gs.washington.edu/), SIFT (http://sift.bii.a-star.edu.sg/) and UMD predictor (http://umd-predictor.eu/), PROVEAN v1.1 (http://provean.jcvi.org/), and MutationAssessor 1.0 (http://mutationassessor.org/r3/). These tools were selected because of their maintenance frequency, estimation congruency, or superior classification records [8, 9]. The potential effect on splice site was assessed using the prediction tool (www.umd.be/HSF3/) [10].

Among all potential pathogenic variants identified in the current datasets, we mainly focused on variants in known causative genes for different forms of PPKs that overlap the patients' clinical features. Based on the OMIM database and the literature review, 18 potential candidates were identified (Table 1) [11]. If no significant sequence variations were detected in these genes, we extended the mutational search to all WES data.

Once likely pathogenic variants were selected, we examined their relation to clinical findings using the VarElect prioritization tool (http://varelect.genecards.org). VarElect uses the Deep LifeMap Knowledgebase to infer direct, as well as indirect, links between genes and phenotypes [12].

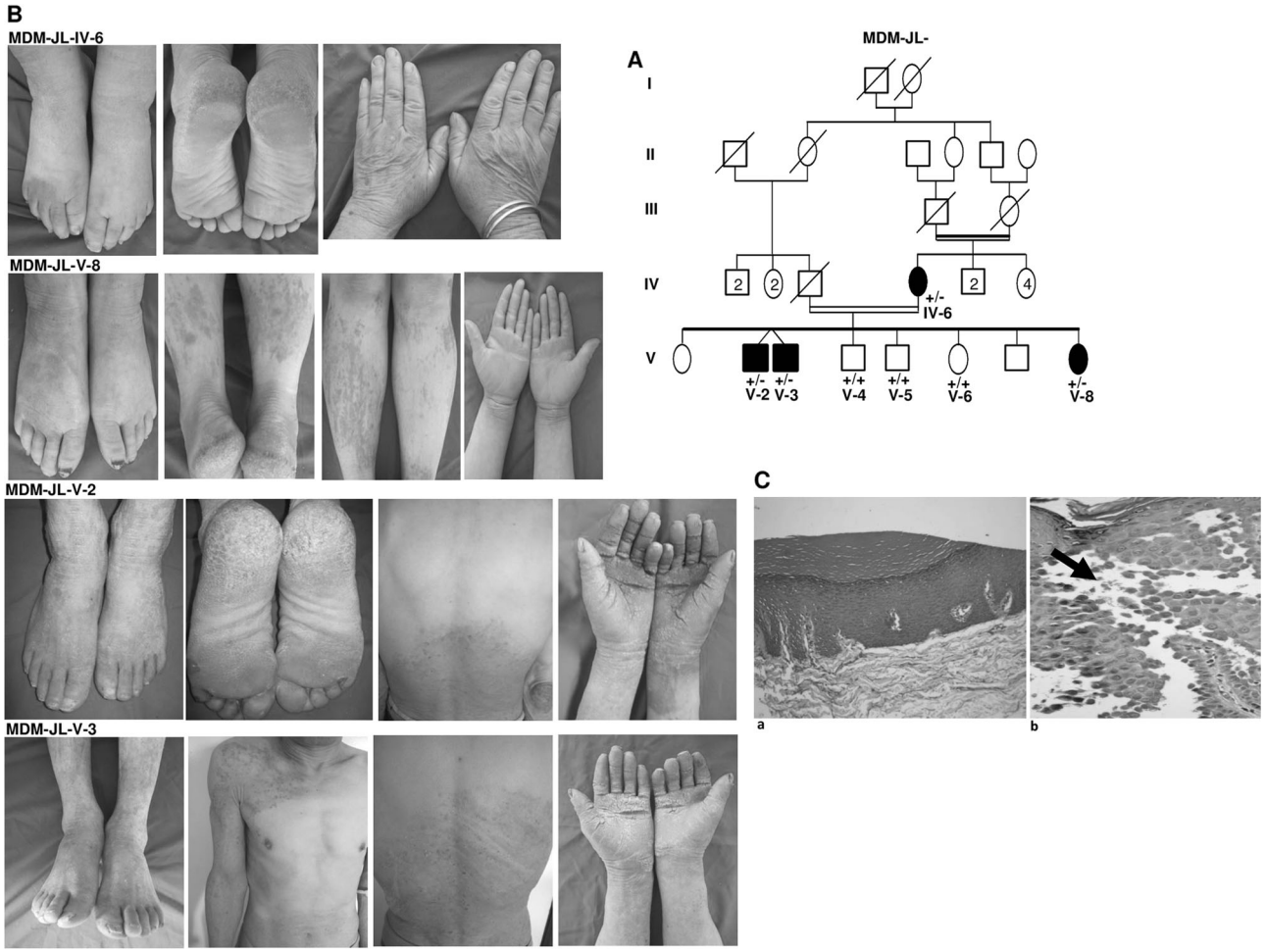

Fig. 1 Pedigree, main clinical and histopathologic features of patients in MDM-JL family. **a** Pedigree of the family segregating with autosomal dominant transgrediens and progrediens PPK. The affected individuals and genotypes of tested family members are indicated. The +/− indicates which individuals had the *CDH12* mutation. **b** Detailed illustrations of the phenotypic features of MDM-JL-IV-6, V-8, V-2, and V3 patients, including the distribution of keratoderma on palms, soles, and other body skin regions. **c** Histopathological findings from biopsy specimens taken from the left palm of patient MDM-JL-V-2 consisted of hyperkeratosis, parakeratosis, hypergranulosis, acanthosis, and hyperpapillomatosis (**a**) (HE, ×100), and from the hyperkeratotic papules of the dorsum of left hand of patient MDM-JL-V-2 showing acantholysis (black arrow) (**b**) (HE, ×400)

DNA Sanger sequencing for variant confirmation

Putative pathogenic variants identified by WES were confirmed in the affected individuals and screened for in unaffected member using standard Sanger sequencing technique. The Primer3 tool (http://bioinfo.ut.ee/primer3-0.4.0/) was used to design the specific primers for PCR amplification and direct sequencing of the surrounding region of the selected candidate causative variants. PCR reactions were performed on genomic DNA, following using automated sequencer (ABI 3500. Applied Biosystems, Foster City, CA) using a cycle sequencing reaction kit (Big Dye Terminator kit, Applied Biosystems). Data were analyzed using BioEdit Sequence Alignment Editor Version 7.2.5.

Protein modeling

To study the effect of a missense mutation on the structure of the human cadherin-12 protein, we used a computational modeling approach. The protein sequence (794 amino acids) was obtained from the UniprotKB database (http://www.uniprot.org accession no: P55289) and no three-dimensional resolved structure was available in the Protein Data Bank. The structure of the extracellular domain (EC) of cadherin-12 (555 amino acids from position 55 to 609) was predicted by Robetta server (http://robetta.bakerlab.org/) using the "Ginzu" domain prediction method [13]. The predicted model was validated through ProSA-web server (https://prosa.services.came.sbg.ac.at/prosa.php), Verify 3D software

Table 1 Differential diagnosis of MDM-JL phenotype

Disease type	Inheritance	Causative gene	Refseq	Onset	Common features to MDM-JL phenotype	Differentiation points
Papillon-Lefevre syndrome	*AR*	***CTSC***	NM_001814	Early childhood	Diffuse, transgrediens PPK	Periodontitis, early tooth loss, T-cell immunodeficiency
Ectodermal dysplasia	*AR*	***PKP1***	NM_000299		Diffuse PPK, nails involvement (dystrophic, hypertrophic, abnormally keratinized)	Skin fragility
Vohwinkel syndrome (classic)	*AD*	***GJB2***	NM_004004	Early childhood	Diffuse, transgrediens and progrediens PPK	Mutilating PPK, deafness, pseudoainhum
Vohwinkel syndrome (variant)		***LOR***	NM_000427	Early childhood	Diffuse, transgrediens and progrediens PPK, erythematous hyperkeratotic plaques	Mutilating PPK, pseudoainhum, honeycomb-like hyperkeratosis, ichthyosiform dermatosis
Thost-Unna or Vorner-type PPK	AD	***KRT1***	NM_006121	Soon after birth to early childhood	Diffuse PPK	Epidermolytic PPK, non-transgredient, rare nail involvement
		KRT9	NM_000226			
Reiter's disease	AD	***KRT1***	NM_006121	Since birth to early childhood	Nonepidermolytic hyperkeratosis, diffuse progrediens and transgrediens PPK	The palms and soles may be spared, rare nail involvement
Bothnian PPK	AD	***AQP5***	NM_001651	Early childhood	Nonepidermolytic hyperkeratosis, diffuse and transgrediens PPK	Nonprogredient, whitish change upon water exposure
Carvajal syndrome	AR	***DSP***	NM_004415	Mostly within infancy	Palmoplantar keratosis, psoriasiform keratosis	Epidermolytic PPK, striate PPK, woolly hair, left ventricle-dilated cardiomyopathy
Naxos disease	AR	***JUP***	NM_002230	Mostly within infancy	Diffuse PPK	Right ventricular dysplasia/ cardiomyopathy, woolly hair
Olmsted syndrome	AR/AD	***TRPV3***	NM_145068	Birth to early childhood	Diffuse and transgrediens PPK, nail involvement	Mutilating PPK, hair involvement, periorificial keratotic plaques
Epidermolysis bullosa simplex localized	AD	***KRT14***	NM_000526	Early childhood	Diffuse PPK	Focal keratoderma of the palms and soles may occur by adulthood
		KRT5	NM_000424			Distribution of PPK in areas of trauma plus blistering
Nagashima-type PPK	AR	***SERPINB7***	NM_003784	Mostly within infancy	Nonepidermolytic hyperkeratosis, diffuse and transgrediens PPK	Nonprogredient, whitish change upon water exposure
Gamborg Nielsen	AR	***SLURP-1***	NM_020427	Soon after birth	Nonepidermolytic PPK	No nails deformities, no hyperhidrosis
Progressive symmetric erythrokeratoderma	AD	***GJB3***	NM_001005752	First year of life Adulthood	Progressive and symmetrical hyperkeratotic plaques over the body, trunck, buttocks, and PPK	No nails abnormalities, no perioral involvement
		GJB4	NM_153212			
		GJA1	NM_000165.4			
Keratosis palmoplantaris striata I PPKSI	AD	***DSG1***	NM_001942	Childhood to adolescence	Diffuse hyperkeratotic lesions on the palms extending along the length of fingers Thick patches of diffuse hyperkeratosis on the soles	Nonprogredient, striate and focal pattern of PPK, no hyperhidrosis

(http://services.mbi.ucla.edu), and RAMPAGE server (http://mordred.bioc.cam.ac.uk/~rapper/rampage.php). PyMOL (version 1.3, http://www.pymol.org/) was used for the structure visualization.

To predict the effects of mutations on protein structure stability, we used two computational approaches: DUET server (http://biosig.unimelb.edu.au/duet/) and I-Mutant3.0 (http://gpcr2.biocomp.unibo.it/cgi/predictors/I-Mutant3.0/I-Mutant3.0.cgi). They allowed us to calculate the Gibbs free energy change (DDG), which is the difference between wild type and mutated protein unfolded Gibbs free energy (DG). A negative value of DDG indicates decrease in protein stability and a positive value indicates increase in protein stability. During the prediction of energy change, the pH and temperature were set respectively as 7 and 25 °C.

Functional annotation and biological network construction

To discern the implication of the *CDH12* candidate gene, several bioinformatics tools have been used to explore its biological pathways and the possible protein–protein (PP) interactions. *CDH12* gene symbol was used as input for the stringdb 11.0 [14] database and GeneMANIA prediction web server [15] for PP interactions including physical and functional association, functional enrichment with GO terms, KEGG pathways, Reactome, Wiki pathway, and network integration for predicting gene function, respectively. All proteins/genes interactions identified using stringdb and geneMANIA were retrieved and integrated into Cytoscape 3.7.2 [16]. We conducted two-sided (enrichment/depletion) hypergeometric distribution tests, with a p value significance level of 0.05, followed by the Bonferroni adjustment using the ClueGO 2.5.4 [17] and CluePedia 1.5.4 [18] plugins of the Cytoscape software [16]. The selection criterion for significantly enriched pathways and GO terms was a p value of 0.05 or less.

Results

Clinical and histological features of affected individuals

Patients V-2, V-3 twin brothers (42 years old) and their V-8 sister (34 years old) were followed up over 13 years in the Dermatology Department of Rabta Hospital for severe progredient and diffuse erythematous PPK. In 2011, during clinical assessment of affected siblings, it was revealed that their mother IV-6 exhibited clinical signs of the disease and was invited at that time for further dermatological examination.

Detailed phenotypic characteristics of the affected family members (IV-6, V-2, V-3, and V-8) are summarized in Table 2. An examination of available medical records of patients (V-2, V-3, and V-8) allowed us to investigate the progression of symptoms and signs over time. The three affected siblings showed a diffuse palmoplantar hyperkeratosis that completely covered the soles and palms and extended in a transgrediens manner to the dorsal surfaces of the hands and feet (Fig. 1b). Hyperkeratotic lesions extending to the sides and the dorsal aspects of the fingers and toes and distinctly demarcated with brownish scaly border from normal skin especially on the palms were characteristic of all affected siblings. In all cases, transgressive pachyderma, an intense hyperhidrosis mainly of the soles and lichenoid plaques on the elbows and knees, were also observed. Various transient lesions such as perioral erythema, angular cheilitis, and erythema of the buttocks were observed during several follow-up visits.

The 67-year-old mother IV-6 exhibited abnormal cornification and a diffuse yellowish keratoderma with the characteristic skin thickening (Fig. 1b). On inquiry, the mother revealed that keratotic lesions started initially when she was 59 years old as small discrete and asymptomatic lesions only in her palms with dominated erythematous component. Over a period of 1 year, they gradually became more hyperkeratotic and extended to the dorsal aspects of the hands and feet. The lesions were more pronounced in areas frequently exposed to mechanical stress. Massive areas of thickening of the palms and soles were also noted over the years.

All patients received treatment with oral retinoids along with topical keratolytics combined with emollients (10% salicylic acid in emulsifying ointment), which was effective in improving their skin condition.

The histopathological examination of lesional palmoplantar skin showed similar pattern including marked hyperkeratosis, parakeratosis, hypergranulosis, and acanthosis without epidermolysis in the epidermis of patients IV-6, V-2, and V-8 (Fig. 1c(a)). Suprabasal acantholysis was also observed in epidermis of patients IV-6 and V-2 (Fig. 1c(b)) suggesting that an acantholytic mechanism might be involved in the disease.

Absence of causative mutations in known mutated PPKs-related genes

Samples from patients MDM-JL-V-2 and V-8, their affected mother (IV-6), and unaffected brother (V-4) were subjected to WES, in order to identify the genetic defect underlying the MDM-JL patients' phenotype. We first investigated the following 18 known causative genes for distinct forms of inherited PPKs that might contribute to MDM-JL patients' phenotype: *CTSC, PKP1, GJB2, LOR, KRT1, KRT9, AQP5, DSP, JUP, TRPV3 KRT14, KRT5 SERPINB7, SLURP-1, GJB3, GJB4, GJA1, and DSG1* (Table 1).

Table 2 Epidemiological and clinical data of affected family members

Patients' characteristics	IV-6	V-2	V-3	V-8
Age (years)	67	42	42	34
Sex	F	M	M	F
Disease onset (years)	59	2	2	3
Pattern of palmoplantar involvement	Bilateral symmetrical diffuse palmoplantar hyperkeratosis Massive, yellowish	Bilateral symmetrical diffuse palmoplantar hyperkeratosis Massive, yellowish	Bilateral symmetrical diffuse palmoplantar hyperkeratosis Massive, greyish	Bilateral symmetrical diffuse palmoplantar hyperkeratosis Massive, yellowish
Transgrediens	Dorsal of hands, feet	Dorsal of hands, feet	Dorsal of hands, feet, ankles	Dorsal of hands, feet, ankles
Progrediens	+	+	+	+
Exfoliative hyperkeratosis with fissures	+	+++	+++	+
Waxy appearance	−	−	−	−
Involvement of other skin areas and/or appendages				
Lichenoid plaques	Elbows, knees	Elbows, knees	Elbows, knees Legs, trunk	Elbows, knees Legs
Hyperkeratotic plaques	The sides and dorsal aspects of fingers, toes demarcated with brownish scaly border	The sides and dorsal aspects of fingers, toes demarcated with brownish scaly border	The sides and dorsal aspects of fingers, toes demarcated with brownish scaly border	The sides and dorsal aspects of fingers, toes demarcated with brownish scaly border
Hyperhidrosis	−	Soles	Soles	Soles
Malodor pachyderma	−	+	+	+
Bacterial infections	−	++	++	+
Fungal infections	−	++	++	+
Nails involvement				
Conical thickening	In distal parts of fingers on both hands	In distal parts of fingers on both hands	In distal parts of fingers on both hands	In distal parts of fingers on both hands
Hyperconvexity	++	+++	+++	++
Dystrophy	Feet	+Hands, feet	+Hands, feet	Feet
Pachyonychia	Toenails	Toenails	Toenails	Toenails
Flexion contractures of the fingers	Hands, feet	Hands, feet	Hands, feet	Hands, feet
Pseudoainhum	−	Second, fifth fingers of both hands	−	−
Perioral erythema	+	+	+	+
Angular cheilitis	−	+ (transient lesions)	+ (transient lesions)	+ (transient lesions)
High arched palate	−	+	+	+
Erythema of the buttocks	−	++ (transient lesions)	++ (transient lesions)	−
Hair/Eyes/Teeth/ Visible mucosae	−	−	−	−

+ patient positive for characteristic, ++ pronounced effect, +++ intense effect, − characteristic not observed

The average read depth across the candidate genes in the three affected family members was 67× with >20 reads for 92% of bases. Only the variants with a read depth greater than 20× were retained. All shared variants among patients MDM-JL-IV-6, V-2, and V-8 were ascertained, and variants with predicted functional consequence were prioritized for analysis. Seven shared heterozygous functional variants were identified of which two relevant nonsynonymous variants were found within the 18 potential candidate genes. These relevant variants corresponded to common exonic polymorphisms on *TRPV3* (rs322937) and *SERPINB7* (rs17782413) genes, previously described in the ExAC database with a respective frequency of 0.34 and 0.21. None of these variants were listed on ClinVar database. Thus, our first genetic analyses showed no potential exonic variant in the 18 tested candidate genes which infers that a novel candidate gene probably is involved in the MDM-JL patients.

Table 3 Variants filtering results of whole-exome sequencing

Inheritance models/Filtering conditions	Autosomal recessive mode	Pseudo-dominant mode	Autosomal dominant mode
	HMZ V-2, V-8 HTZ IV-6	HMZ IV-6, HMZ V-2, V-8	HTZ IV-6, V-2, V-8 Abs V-4
Total number of variants	2503	16,480	5359
Relevants variants: Missense, nonsense, splice-site or frameshift variants	367	2896	675
Frequency (MAF < 0.01) dbSNP ExAC 1000 genomes	2	12	112
Prediction in silico MutationTaster PolyPhen CADD > 15 SIFT UMD predictor PROVEAN v1.1 MutationAssessor 1.0	0	1 (*BYSL* NM_004053: exon2 c.431 + 3A > G) rs188902641 (human splicing finder)	19
Phenotype-prioritization tool	0	0	1 (*CDH12* NM_004061: exon 5, c.1655C > A, p.Thr552Asn)

Identification of novel rare potentially candidate variant for MDM-JL's phenotype

We extended the mutational search to all WES data. Given the known consanguinity in this family, we expected a homozygous mutation causing the disease. However, based on family history and genealogical tree, we hypothesized that both pseudo-dominant and dominant patterns of inheritance could occur (Fig. 1a). A summary of the bioinformatic workflow of this study is presented in Table 3. Briefly, variants identified as intronic, intergenic, and none coding or synonymous were discarded. Assuming that causative variants are rare, we removed all variants with MAF >1% in the dbSNP, ExAC, and 1000 genomes databases. To narrow down the range of candidate variants, we used six bioinformatics tools to predict the potential pathogenicity of variants. Finally, significant candidate variants were obtained after filtering against their phenotypic relevance. To test possible pseudo-dominant inheritance, homozygous variants among patients MDM-JL-IV-6, V-2, and V-8 were selected. Twelve shared rare homozygous variants were identified in the affected individuals. They corresponded to 11 nonsynonymous and one splice acceptor site mutation (Table 3), but none was predicted to be pathogenic.

We then considered an autosomal dominant inheritance with full penetrance, and selected heterozygous variants present in all affected individuals, but not in the unaffected sibling. A total of 5359 variants were identified (Table 3). Among them, 675 heterozygous, exonic, splicing variants, and nonsynonymous variants were called. In the next step, 112 rare variants were selected for further investigations. Among them, a list of 19 high candidate variants within eight different genes were selected based on interesting in silico prediction (Table 4) of which 15 nonsynonymous variants on *ZNF806*. *ALPI*, *CDH12*, three splicing variations on *SP100*, *ZFC3H1*, *SKA3*, and 1 frameshift insertion on *C17orf107*. None of these variants were classified in ClinVar database. However, two high risk unreported variants within *ALPI* and *CDH12* genes were predicted as "damaging" by SIFT and PolyPhen-2 and as "disease causing" by MutationTaster tools. Subsequently, we applied VarElect using the relevant keywords "PPK" and "transgrediens" in order to obtain a ranked list of the eight candidate genes. The *CDH12* gene (NM_004061; 5p14.3), which has never been involved in genodermatosis, had the highest score according to VarElect (score = 40.03). The *CDH12* gene encodes for a neural cadherin (N-cadherin 2, cadherin-12), a type II classical cadherin that is a member of the calcium-dependent cell–cell adhesion cadherin superfamily [19]. Like other members of classical cadherins (e.g., E-, VE- and P-cadherins), cadherin-12 share a common modular structure composed an EC containing 5 extracellular cadherin (EC) repeats (aa 1–609) responsible for

Table 4 List of variants identified after the filtering process according to the autosomal dominant pattern of inheritance

Chr	Position	Gene	RefSeq	Coding change	Variant type	dbSNP ID	Frequency	SIFT	PolyPhen-2	MutationTaster	Clinvar
2	133074876	ZNF806	NM_001304449	c.337A > G:p.M113V	Nonsynonymous	rs7355689	NA	NA	NA	NA	NA
2	133075027	ZNF806	NM_001304449	c.488G > A:p.G163E	Nonsynonymous	rs7349198	NA	NA	NA	NA	NA
2	133075104	ZNF806	NM_001304449	c.565C > T:p.R189C	Nonsynonymous	rs7349364	0.00008	NA	NA	NA	NA
2	133075207	ZNF806	NM_001304449	c.668C > T:p.A223V	Nonsynonymous	rs7349365	0.000399361	NA	NA	NA	NA
2	133075282	ZNF806	NM_001304449	c.743T > C:p.V248A	Nonsynonymous	rs7349446	NA	NA	NA	NA	NA
2	133075365	ZNF806	NM_001304449	c.826G > A:p.V276I	Nonsynonymous	rs7349215	NA	NA	NA	NA	NA
2	133075386	ZNF806	NM_001304449	c.847G > A:p.G283R	Nonsynonymous	rs7349216	0.00001	NA	NA	NA	NA
2	133075639	ZNF806	NM_001304449	c.1100G > T:p.G367V	Nonsynonymous	rs7340191	NA	NA	NA	NA	NA
2	133075664	ZNF806	NM_001304449	c.1125T > G:p.D375E	Nonsynonymous	rs7340499	NA	NA	NA	NA	NA
2	133075674	ZNF806	NM_001304449	c.1135G > C:p.G379R	Nonsynonymous	rs7340192	NA	NA	NA	NA	NA
2	133076032	ZNF806	NM_001304449	c.1493T > G:p.F498C	Nonsynonymous	rs2598809	NA	NA	NA	NA	NA
2	133076206	ZNF806	NM_001304449	c.1667C> T:p.A556V	Nonsynonymous	rs2598807	0.000008	NA	NA	NA	NA
2	231363253	SP100	NM_001080391	c.1720 + 3- > A	Splicing	NA	NA	NA	NA	NA	NA
2	233321937	ALPI	NM_001631	c.553C > T:p.R185C	Nonsynonymous	NA	NA	Damaging	Damaging	Disease causing	NA
5	21755930	CDH12	NM_004061	c.1655C > A:p.T552N	Nonsynonymous	NA	NA	Damaging	Damaging	Disease causing	NA
12	72028608	ZFC3H1	NM_144982	c.2239-3- > T	Splicing	NA	NA	NA	NA	NA	NA
13	21729953	SKA3	NM_145061	c.1120-3- > T	Splicing	NA	NA	NA	NA	NA	NA
17	4803299	C17orf107	NM_001145536	c.136dupC:p.E45fs	Frameshift insertion	rs201204280	0.0018	NA	NA	NA	NA
22	51159722	SHANK3	NM_033517	c.3419G > A:p.G1140E	Nonsynonymous	NA	NA	NA	NA	NA	NA

ZNF806 may function as a transcription factor. *SP100* gene encodes a subnuclear organelle and major component of the PML (promyelocytic leukemia). *ALPI* gene encodes the human alkaline phosphatase intestinal that is an enzyme involved in the gut mucosal defense system and is thought to function in the detoxification of lipopolysaccharide, and in the prevention of bacterial translocation in the gut. *CDH12* gene encodes a cadherin calcium-cell adhesion protein. *ZFC3H1* gene encodes for a subunit of the trimeric poly(A) tail exosome targeting complex. *SKA3* gene encodes a component of the spindle and kinetochore-associated protein complex that regulates microtubule attachment to the kinetochores during mitosis. *C17orf107* uncharacterized function. *SHANK3* gene encodes a major scaffold postsynaptic density protein that interacts with multiple proteins and complexes to orchestrate the dendritic spine and synapse formation, maturation and maintenance

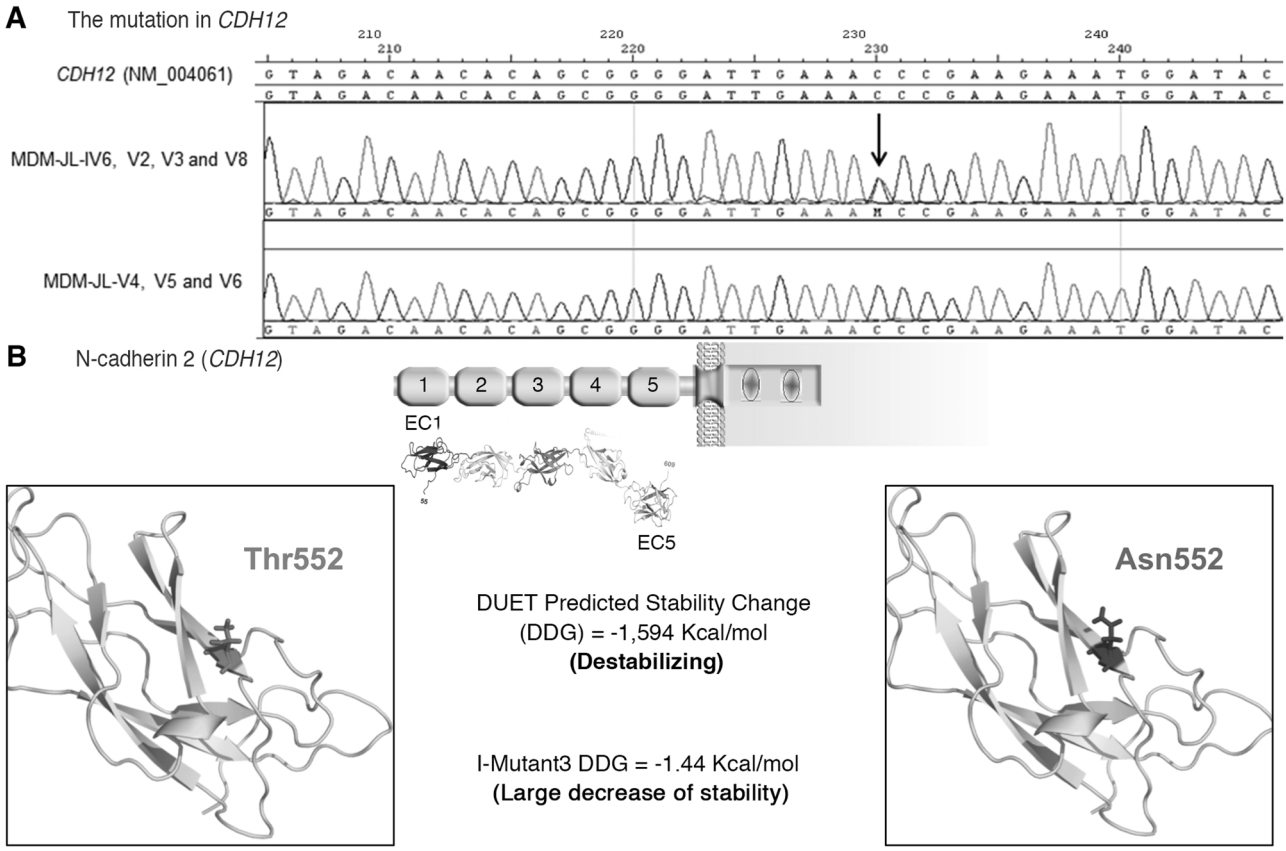

Fig. 2 Identification and characterization of the novel variant (c.1655C > A, p.Thr552Asn) on *CDH12* gene. **a** DNA-sequence of the cadherin-12 gene (*CDH12*) (NM_004061) showing the novel heterozygous (c.1655C > A, p.Thr552Asn) variant identified in the patients (MDM-JL V-2, 3, and 8) compared with unaffected family member (MDM-JL-V-4). **b** Domain structure of N-cadherin 2/cadherin-12, and modeling of the extracellular cadherin (EC) domain with the *CDH23* mutation. Upper panel: cadherin-2 consists three segments, i.e., an extracellular domain EC 1–5 (55–609), a transmembrane domain (610–637), and a conserved cytoplasmic domain (638–794) that interacts with two catenins, p120-catenin and ß-catenin. Lower panels: a model of the extracellular region of cadherin-12 (amino acids 55–609) obtained from Robetta and showing five EC domains. The EC5 domain (green) is zoomed to show the Threonine (Thr) at position 552 (red stick) mutated to Asparagine (Asn, blue sticks). DUET and I-mutant3 scores showed that the p.Thr552Asn mutation will result in a protein destabilization

cadherin–cadherin interactions, a transmembrane (TM) domain (aa 610–637), and a conserved cytoplasmic domain (aa 638–794) that interacts with various proteins, collectively termed catenins, that link cadherins to the actin-based cytoskeleton (see also Fig. 2b) [19]. According to the Human Protein Atlas, CDH12 is effectively expressed in skin, with medium and high expression found in keratinocytes and epidermal cells, respectively (https://www.proteinatlas.org/ENSG00000154162-CDH12/tissue/skin). Together, these data prompted us to further study the pathogenicity of the *CDH12* mutation. The heterozygous nonsynonymous variant (c.1655C > A, p.Thr552Asn) found in the *CDH12* gene was present in all affected family members but was absent in the unaffected sibling and therefore represented a potential disease-causing variant (Fig. 2a). Finally, direct sequencing confirmed the presence of this variant at heterozygous state in affected individuals (MDM-JL-IV-6, V-2, V-3, and V-8) and its absence in the nonaffected siblings (MDM-JL-V-4, 5, and 6), suggesting an autosomal dominant inheritance with full penetrance as the most likely inheritance pattern. In addition, the (c.1655C > A, p.Thr552Asn) variant was absent in dbSNP and in 50 in-house control exomes, thus indicating that the mutation was not a polymorphism.

In silico mutation prediction and structure modeling

The p.Thr552Asn (NP_004052.2) variant on *CDH12* gene was predicted to be deleterious by SIFT, damaging by PolyPhen-2, and disease causing by MutationTaster. The structure of the EC of the cadherin-12 (aa 55–609) was modeled by Robetta server (Fig. 2b). The overall quality of the model was assessed using ProSA server with the quality index represented by a *Z*-score of −8.04, which is within the range of scores found in experimental protein structures of similar size. The structure was also validated by Verify 3D software showing that 80.54% of the residues had an average 3D–1D score ≥0.2. The Ramachandran plot

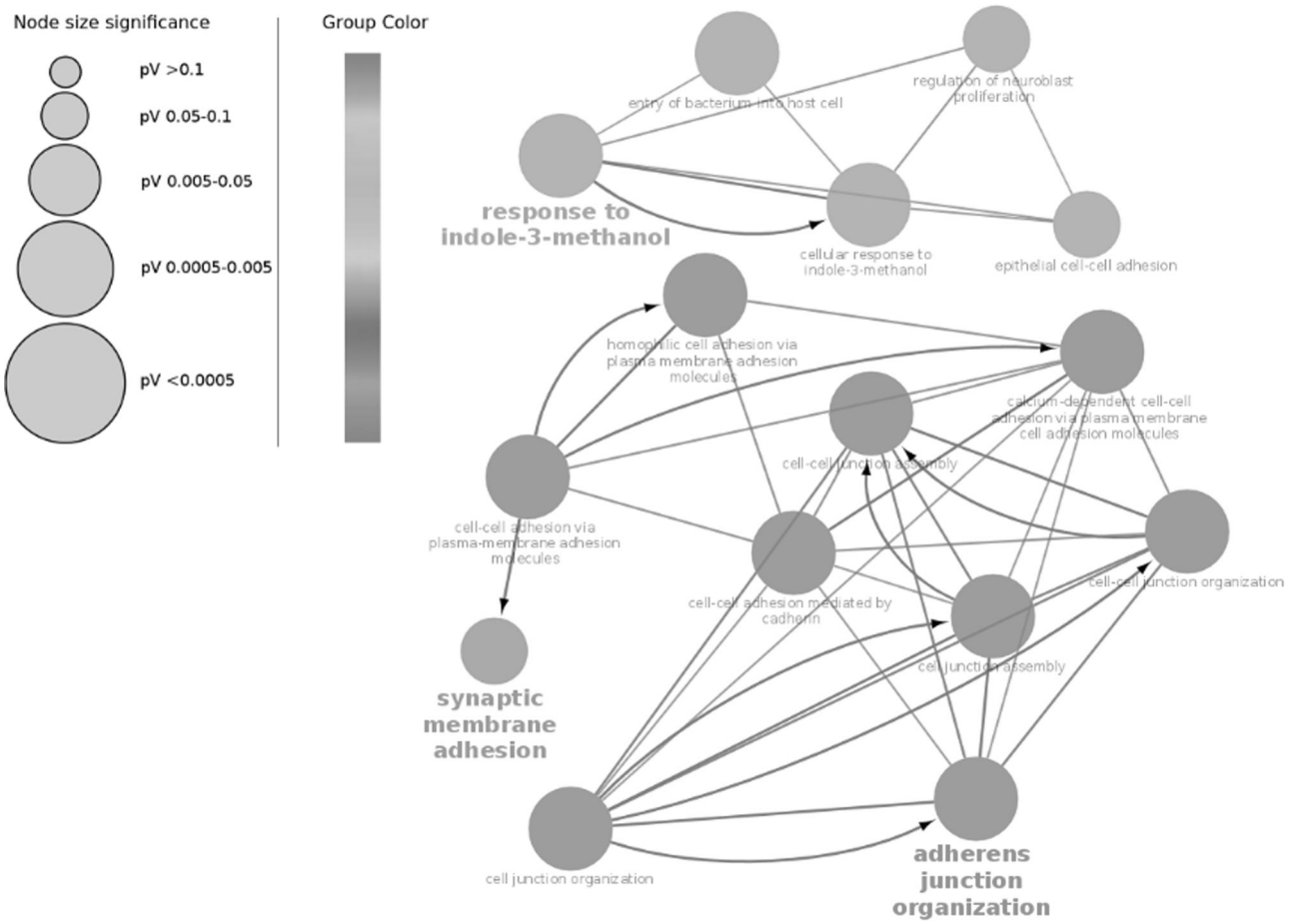

Fig. 3 Protein-protein interaction networks related to CDH12 identified with Stringdb 11.0 database and GeneMANIA prediction web server

analysis of this model structure showed 98.6% of residues in favored region, 1.3% in allowed region, and 0.2% in outlier region. DUET and I-Mutant3 servers were used to assess the energetic consequences of p.Thr552Asn substitution on the cadherin-12 predicted model. The DDG calculation revealed that the mutation decreases the stability of the protein (Mutant3.0 DDG = −1.44 Kcal/mol and DUET DDG = −1.594 Kcal/mol) (Fig. 2b).

Overall, the tools provide an additional in silico support for the consideration of the p.Thr552Asn mutation in *CDH12* gene as likely pathogenic rather than a rare benign polymorphism.

Functional annotation analysis

PP interactions network related to CDH12 identified with Stringdb and GeneMania are highlighted in Fig. 3. GO biological process terms enrichment using stringdb 11.0 database showed that the CDH12 PPI network is significantly associated with adherens junction (AJ) organization (FDR = 5.42e−24), cell–cell junction organization (FDR = 1.41e−20), cell–cell adhesion (FDR = 1.41e−20), and homophilic cell adhesion via plasma membrane adhesion molecules (FDR = 1.25e−10). GO molecular function terms that are highly enriched include calcium ion binding (FDR = 5.43e−07), binding (FDR = 0.0282) while those highly associated with GO cellular components terms are plasma membrane (FDR = 6.72e−06), membrane part (FDR = 0.00077), and intrinsic component of membrane (FDR = 0.0430). All enriched GO biological processes are highlighted in Fig. 4a, b using ClueGO 2.5.4 tool [17].

Results showed that CDH12 interacts with different members of the cadherin superfamily involved in several pathways: cell–cell adhesion (CDH1, CDH7), cell–cell AJ (CDH18, CDH9), and cell–cell junction organization (CDH17, CTNNB1, CTNND1, CDH24). The CDH12 protein directly interacts with JUP protein that is expressed in skin and involved with desmosome in AJs organization.

Discussion

We report here a detailed clinical and genetic characterization of a consanguineous Tunisian family (MDM-JL)

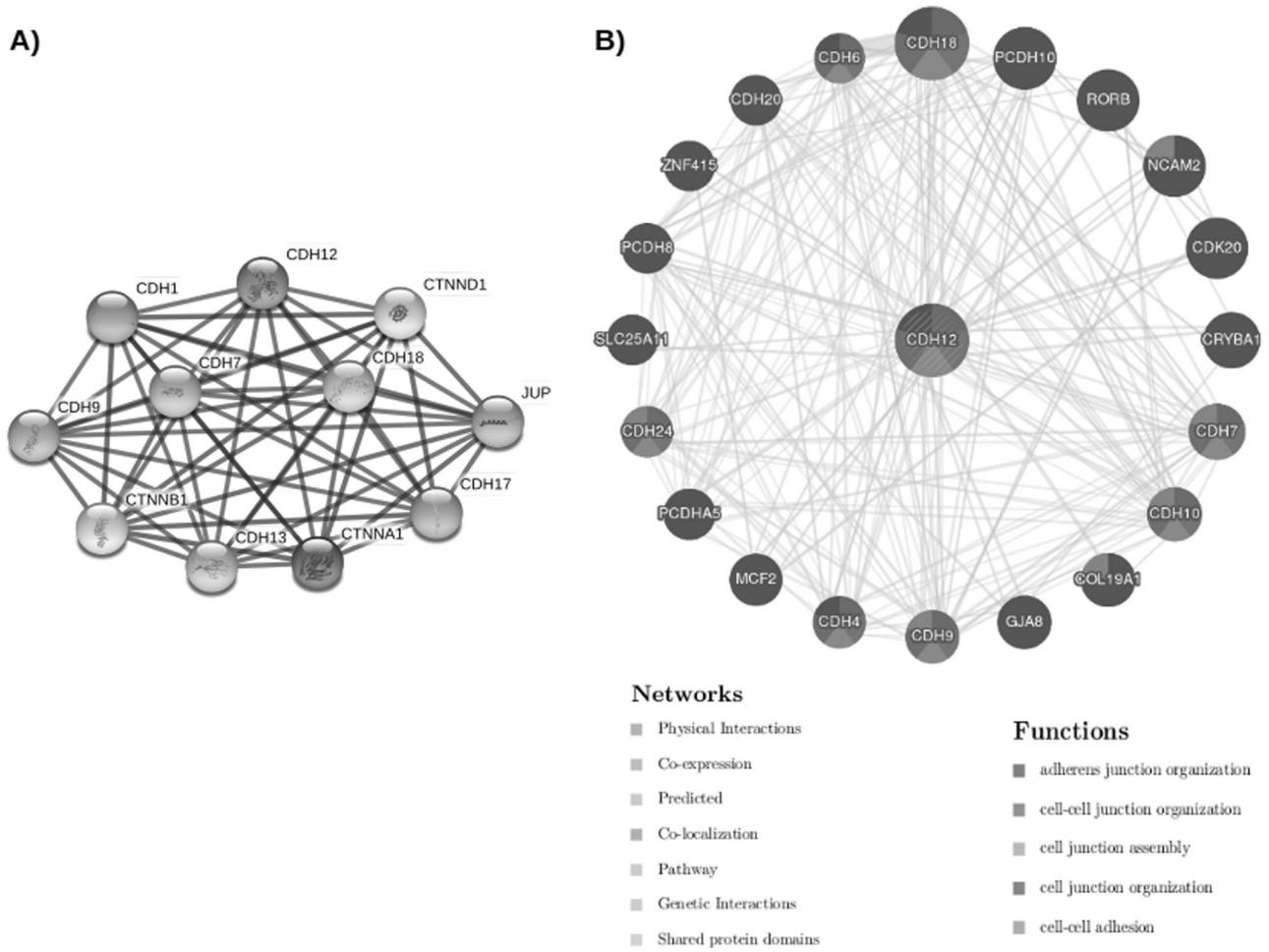

Fig. 4 Biological process enrichment of the CDH12 protein–protein interaction networks using ClueGO 2.5.4

with atypical clinical presentation of inherited PPK. Three affected siblings of this family have already been documented by our study group as having MDM-like autosomal recessive PPK unlinked to *SLURP-1*, suggesting that genetic heterogeneity may exist in MDM, or there is at least one other phenotypic variant of MDM caused by mutations in a different gene. After a follow up of 13 years, our further reinvestigation of this family revealed that the mother developed similar expression of the disease, which raised the question of whether the PPK phenotype exhibited by affected members of MDM-JL family is distinct from other known inherited forms of PPK that may involve clinical expression in adulthood. The main clinical findings of MDM-JL patients' phenotype include transgressive and progressive PPK associated with lichenoid or keratotic plaques on the elbows and knees, perioral erythema, nail involvement, and hyperhydrosis. This phenotype can be differentiated from other inherited PPKs based on many clinical criteria. Syndromic transgressive PPK such as Naxos disease (MIM 601214), Papillon–Lefèvre syndrome (MIM 248300), the classic form of Vohwinkel syndrome (MIM 124500), or the variant form with ichthyosis (MIM 604117) were ruled out based on the absence of characteristic clinical features. The Gamborg Nielsen-type (MIM 244850) shows a simila, but less severe phenotype than in MDM, i.e., a milder hyperkeratosis, no nail dystrophies or lichenoid plaques and no pachydermia or distant keratosis [20]. However, all patients in this family displayed nail changes and lichenoid plaques on elbows and knees that are not consistent with the Gamborg Nielsen PPK type. The MDM-JL patients' phenotype resembles Nagashima-type PPK (MIM 615598) in terms of its hyperkeratosis with transgrediens and hyperhidrosis but it differs clinically based on the non-progressive nature of the hyperkeratosis and also the absence of flexion contractures or constricting bands [21]. Greither's disease (MIM 144200) has also several clinical similarities with symptoms observed in MDM-JL patients, specifically the presence of hyperkeratosis of knees and elbows, which is considered as a typical finding of Greither's PPK. However, in contrast to MDM disease and to MDM-JL patients' phenotype, the palms and soles may be spared in Greither's disease [22].

The coexistence of localized hyperkeratotic areas over the extensor surface of the joints with underlying erythema and the symmetrical distribution of lesions observed in MDM-JL patients led us to suspect the diagnostic of progressive symmetric erythrokeratoderma (PSEK, MIM 602036). PSEK is a rare cornification disorder characterized by symmetric and progressive erythematous hyperkeratotic patches over the body, particularly on the trunk and limbs, buttocks, and face often associated with a greater clinical expression of PPK [23, 24]. The phenotype is usually present at birth or develops during the first year of life, but delayed onset of the condition as late as adulthood has also been described [25]. Among 25 patients with PSEK reported in the study of Wei et al. [26], 60% of them developed lesions in adulthood and 92% exhibited PPK [26]. The severity and progression of the PSEK disorder can vary greatly from one person to another, even among members of the same family [27]. In some families, PSEK can be part of the clinical spectrum of other rare skin disorders, such as erythrokeratodermia variabilis (MIM 133200) or loricrin keratoderma [28, 29]. Furthermore, Bouadjar et al. have suggested that MDM phenotype might, in some cases, be confused with PSEK [30]. Progressive nature of the lesions, symmetrical distribution of hyperkeratotic lesions associated with the presence of diffuse PPK, and adulthood expression noted in MDM-JL family support the possible diagnosis of PSEK. Nevertheless, nails abnormalities and perioral involvement that were observed in our patients are not usual findings of the PSEK phenotype. Consequently, we suggest that they might have a new phenotype similar to PSEK.

To determine the molecular etiology of the MDM-JL patients' phenotype, we performed WES for two affected cases (JL-V-2 and JL-V-8), affected mother (JL-IV-6), and unaffected sibs (JL-V-4, 5, and 6). Our analysis first focused on variants located in a list of candidate genes (Table 1). These genes are associated with various functions including structural stabilization (keratins, loricrin, transglutaminase, ichthyin), cell adhesion (plakophilin, desmoplakin, desmoglein 1), cell-to-cell communication (connexins), and TM signal transduction (cathepsin C) [31, 32]. The partial clinical overlap with PSEK features prompted us to screen *GJB3* (Cx31), *GJB4* (Cx30.3), and *GJA1* (Cx43) genes involved in the etiology of the disease [28, 33–35]. We found no potentially functional rare variants in known PPKs- or PSEK-related genes, indicating the implication of another disease gene in MDM-JL family.

We then extended the mutational search to all WES data for the three patients. Consistent with an autosomal dominant inheritance, two novel heterozygous potentially pathogenic variants within *APLI* and *CDH12* genes were identified. The *APLI* gene encodes an alkaline phosphatase intestinal enzyme that is expressed at a high concentration in the brush border membrane of intestinal epithelial cells. Recent reviews have highlighted the importance of intestinal-type ALP in gut homeostasis. Intestinal-type ALP controls bacterial endotoxin-induced inflammation by dephosphorylating lipopolysaccharide and is a gut mucosal defense factor [36]. Therefore, the *APLI* gene is unlikely to be a candidate disease gene for MDM-JL patients' phenotype. Another novel likely pathogenic heterozygous variant (c.1655C > A, p.Thr552Asn) within *CDH12* gene was identified in MDM-JL family. This mutation was confirmed by Sanger sequencing and fully cosegregated with the phenotype (Fig. 2a). *CDH12* has been associated with bipolar disease and schizophrenia, as well as with methamphetamine and alcohol dependency [37]. Recently, *CDH12* has also been reported as a prognostic factor in colorectal cancer (CRC) patients and plays an oncogenic role in CRC cells [38]. To date, apart from this study, no data are available regarding a possible involvement of the *CDH12* gene in the pathogenesis of PPK or any other genodermatosis. Previous studies have reported mutations in P-cadherin and E-cadherin genes as the cause of several severe skin diseases [39]. Indeed, cadherins' mediated organization of epidermal cell–cell adhesion and the formation of AJs in the epidermis are essential to develop and maintain epidermis full barrier activity [40]. Previous studies have demonstrated that exogenous expression of various mutant N-cadherins, whose EC was largely deleted, in *Xenopus* embryos and in mouse keratinocytes, caused disruption of epithelial cell–cell adhesion [41]. These observations highlight the crucial role of functional N-cadherin and their conserved ECs in cadherin mediated cell–cell adhesion system.

The p.Thr552Asn variant in the *CDH12*, localized in the EC domain (EC5), which is involved in mediating calcium-dependent adhesive interactions, might interfere with the protein function and affects cell–cell adhesion in skin cellular compartments. In silico analysis predicted that this mutation would probably decrease the stability of the protein (Fig. 2b), which in turn might lead to functional alteration of cellular activity and adhesion. Therefore, it is very likely that a defect in cadherin-12 might disturb its adhesive properties thus interfering with cell–cell adhesion in skin. The histological findings of the acantholysis of part of the hyperkeratotic epidermis with hyperkeratosis observed in patients (IV-6 and V-8) demonstrated respectively a loss of intercellular adhesion between keratinocytes and a massive keratinocytes hyperproliferation associated with the disease phenotype in MDM-JL family. These histological features are in accordance with an altered process of intercellular cohesion between keratinocytes resulting in cell separation and rounded cellular outline (Fig. 1c).

Few experimental studies have explored the levels expression of CDH12 others than in brain, colorectal carcinoma tissues, and salivary adenoid cystic carcinoma [38]. However, Human Protein Atlas database and other databases indicate that CDH12 is expressed in various tissue types including skin. Immunohistochemical analysis using an anti-CDH12 antibody in biopsy specimen obtained from the skin demonstrated a

strong staining of stratum granulosum of keratinocytes that corresponds to the superficial layer closest to keratinized layer of epidermis. This observation provides further supporting evidence for the involvement of CDH12 in the process of cornification in the human skin [42]. Moreover, in a study from Yin et al., microarray analysis of skin suction blisters from African, Asian, and Caucasian subjects revealed a differential epidermal gene expression profile between the three distinct ethnic groups. Among the genes differentially expressed, the *CDH12* was found as significantly differentially expressed (>1.5 fold) between the three types of skin [43]. The *CDH12* gene was already reported to be involved with the regulation of skin color, nevertheless, further studies will be needed to assess its functional role in the skin phenotype [44].

Enriched biological process and PP interaction networks further support our hypothesis that *CDH12* gene is likely a relevant functional candidate gene as it plays a role in the AJ organization and cell–cell adhesion junction assembly involved in the maintenance of the normal tissue architecture (Figs. 3 and 4).

In conclusion, we here report a large consanguineous family with an atypical presentation of an autosomal dominant form of transgrediens and progrediens PPK. Our genetic and in silico analyses suggest that (*CDH12*, c.1655C > A, p.Thr552Asn) might be the causative rare variant for this phenotype. Functional annotation data provide further supporting evidence for the potential role of *CDH12* in the maintenance of skin integrity.

The variability in the age at onset among affected members highlights the importance of a long follow up and examining parents and multiple family members even in the absence of skin symptoms at the first clinical presentation. Moreover, dermatologists should be aware that initial manifestation during adulthood does not exclude the possibility of a hereditary PPK.

While in silico predictions support the pathogenicity of the identified mutation in *CDH12* gene, additional functional assays are needed to experimentally assess the effects of (c.1655C > A, p.Thr552Asn) mutation in *CDH12* gene. This gene should be considered as a potential candidate for PPK-related phenotypes. Confirmation of its involvement in hereditary PPK is also important to elucidate the molecular mechanisms of epidermal differentiation in palms and soles, ultimately leading to targeted corrective therapies.

Acknowledgements We would like to warmly acknowledge the patients and their families for their collaboration and all clinicians involved the care of the patients.

Funding This work was supported by the Tunisian Ministry of Public Health, the Ministry of Higher Education and Scientific Research (LR16IPT05), and RARE-MED project (A* MIDEX Initiative d'excellence). The funders had no role in the study design, data collection and analysis, decision to publish, or preparation of the manuscript.

Compliance with ethical standards

Conflict of interest The authors declare that they have no conflict of interest.

Publisher's note Springer Nature remains neutral with regard to jurisdictional claims in published maps and institutional affiliations.

References

1. Botstein D, Risch N. Discovering genotypes underlying human phenotypes: past successes for mendelian disease, future approaches for complex disease. Nat Genet. 2003;33:228–37. http://www.ncbi.nlm.nih.gov/pubmed/12610532.
2. Lai-Cheong JE, McGrath JA. Next-generation diagnostics for inherited skin disorders. J Investig Dermatol. 2011;131:1971–3. https://linkinghub.elsevier.com/retrieve/pii/S0022202X15350557.
3. Hsu TM, Kwok PY. Advances in molecular medicine. J Am Acad Dermatol. 2001;44:847–55. http://linkinghub.elsevier.com/retrieve/pii/S0190962201537731.
4. Kimyai-Asadi A, Kotcher LB, Jih MH. The molecular basis of hereditary palmoplantar keratodermas. J Am Acad Dermatol. 2002;47:327–43. http://www.ncbi.nlm.nih.gov/pubmed/12196741.
5. Bchetnia M, Charfeddine C, Kassar S, Zribi H, Guettiti HT, Ellouze F, et al. Clinical and mutational heterogeneity of Darier disease in Tunisian Families. Arch Dermatol. 2009;145. https://doi.org/10.1001/archdermatol.2009.52.
6. Bchetnia M, Laroussi N, Youssef M, Charfeddine C, Ben Brick AS, Boubaker MS, et al. Particular Mal de Meleda phenotypes in Tunisia and mutations founder effect in the Mediterranean region. Biomed Res Int. 2013;2013:1–7. http://www.hindawi.com/journals/bmri/2013/206803/.
7. Charfeddine C, Mokni M, Kassar S, Zribi H, Bouchlaka C, Boubaker S, et al. Further evidence of the clinical and genetic heterogeneity of recessive transgressive PPK in the Mediterranean region. J Hum Genet. 2006;51:841–5. https://doi.org/10.1007/s10038-006-0002-8.
8. Castellana S, Mazza T. Congruency in the prediction of pathogenic missense mutations: state-of-the-art web-based tools. Brief Bioinform. 2013;14:448–59. http://www.ncbi.nlm.nih.gov/pubmed/23505257.
9. Castellana S, Fusilli C, Mazza T. A broad overview of computational methods for predicting the pathophysiological effects of non-synonymous variants. 2016; 423–40. http://link.springer.com/10.1007/978-1-4939-3572-7_22.
10. Desmet F-O, Hamroun D, Lalande M, Collod-Béroud G, Claustres M, Béroud C. Human splicing finder: an online bioinformatics tool to predict splicing signals. Nucleic Acids Res. 2009;37:e67. https://doi.org/10.1093/nar/gkp215.
11. Has C, Technau-Hafsi K. Palmoplantar keratodermas: clinical and genetic aspects. J der Dtsch Dermatologischen Ges. 2016;14:123–40. http://www.ncbi.nlm.nih.gov/pubmed/26819106.
12. Stelzer G, Plaschkes I, Oz-Levi D, Alkelai A, Olender T, Zimmerman S, et al. VarElect: the phenotype-based variation prioritizer of the GeneCards Suite. BMC Genom. 2016;17 Suppl 2:444. http://bmcgenomics.biomedcentral.com/articles/10.1186/s12864-016-2722-2.
13. Chivian D, Kim DE, Malmström L, Bradley P, Robertson T, Murphy P, et al. Automated prediction of CASP-5 structures using the Robetta server. Proteins. 2003;53 Suppl 6:524–33. https://doi.org/10.1002/prot.10529.
14. Szklarczyk D, Gable AL, Lyon D, Junge A, Wyder S, Huerta-Cepas J, et al. STRING v11: protein-protein association networks

with increased coverage, supporting functional discovery in genome-wide experimental datasets. Nucleic Acids Res. 2019;47: D607–13.
15. Warde-Farley D, Donaldson SL, Comes O, Zuberi K, Badrawi R, Chao P, et al. The GeneMANIA prediction server: biological network integration for gene prioritization and predicting gene function. Nucleic Acids Res. 2010;38 Suppl 2: (Web Server issue) W214–W220.
16. Shannon P, Markiel A, Ozier O, Baliga NS, Wang JT, Ramage D, et al. Cytoscape: a software environment for integrated models of biomolecular interaction networks. Genome Res. 2003; 13:2498–504.
17. Bindea G, Mlecnik B, Hackl H, Charoentong P, Tosolini M, Kirilovsky A, et al. ClueGO: a cytoscape plug-in to decipher functionally grouped gene ontology and pathway annotation networks. Bioinformatics. 2009;25:1091–3. http://www.ncbi.nlm.nih.gov/pubmed/19237447.
18. Bindea G, Galon J, Mlecnik B. CluePedia cytoscape plugin: pathway insights using integrated experimental and in silico data. Bioinformatics. 2013;29:661–3. http://www.ncbi.nlm.nih.gov/pubmed/23325622.
19. Shapiro L, Weis WI. Structure and biochemistry of cadherins and catenins. Cold Spring Harb Perspect Biol. 2009;1:a003053. https://doi.org/10.1101/cshperspect.a003053.
20. Zhao L, Vahlquist A, Virtanen M, Wennerstrand L, Lind L, Lundström A, et al. Palmoplantar keratoderma of the Gamborg-Nielsen type is caused by mutations in the SLURP1 gene and represents a variant of Mal de Meleda. Acta Derm Venereol. 2014;94:707–10. http://www.ncbi.nlm.nih.gov/pubmed/24604124.
21. Kubo A. Nagashima-type palmoplantar keratosis: a common Asian type caused by SERPINB7 protease inhibitor deficiency. J Investig Dermatol. 2014;134:2076–9. https://linkinghub.elsevier.com/retrieve/pii/S0022202X15369499.
22. Athanikar SB, Inamadar AC, Palit A, Sampagavi VV, Deshmukh NS. Greither's disease. Indian J Dermatol Venereol Leprol.2003; 69:292–3. http://www.ncbi.nlm.nih.gov/pubmed/17642916.
23. Duchatelet S, Hovnanian A. Erythrokeratodermia variabilis et progressiva allelic to oculo-dento-digital dysplasia. J Investig Dermatol. 2015;135:1475–8. https://linkinghub.elsevier.com/retrieve/pii/S0022202X15372687.
24. Mahajan V, Khatri G, Chauhan P, Mehta K, Raina R, Gupta M. Progressive symmetric erythrokeratoderma having overlapping features with erythrokeratoderma variabilis and lesional hypertrichosis: is nomenclature "erythrokeratoderma variabilis progressiva" more appropriate? Indian J Dermatol. 2015;60:410 http://www.ncbi.nlm.nih.gov/pubmed/26288417.
25. Prabhu S, Shenoi SD, Pai SB, Handattu S, Bhattachan B. Progressive and symmetric erythrokeratoderma of adult onset: a rare case. Indian Dermatol Online J. 2010;1:43–5. http://www.idoj.in/text.asp?2010/1/1/43/73261.
26. Wei S, Zhou Y, Zhang TD, Huang ZM, Zhang XB, Zhu HL, et al. Evidence for the absence of mutations at GJB3, GJB4 and LOR in progressive symmetrical erythrokeratodermia. Clin Exp Dermatol. 2011;36:399–405. https://doi.org/10.1111/j.1365-2230.2010.03974.x.
27. Common JEA, O'Toole EA, Leigh IM, Thomas A, Griffiths WAD, Venning V, et al. Clinical and genetic heterogeneity of erythrokeratoderma variabilis. J Investig Dermatol. 2005;125:920–7. https://linkinghub.elsevier.com/retrieve/pii/S0022202X15325069.
28. van Steensel MAM, Oranje AP, van der Schroeff JG, Wagner A, van Geel M. The missense mutation G12D in connexin30.3 can cause both erythrokeratodermia variabilis of Mendes da Costa and progressive symmetric erythrokeratodermia of Gottron. Am J Med Genet A. 2009;149A:657–61. https://doi.org/10.1002/ajmg.a.32744.
29. Ishida-Yamamoto A. Loricrin keratoderma: a novel disease entity characterized by nuclear accumulation of mutant loricrin. J Dermatol Sci. 2003;31:3–8. http://www.ncbi.nlm.nih.gov/pubmed/12615358.
30. Bouadjar B, Benmazouzia S, Prud'homme JF, Cure S, Fischer J. Clinical and genetic studies of 3 large, consanguineous, Algerian families with Mal de Meleda. Arch Dermatol. 2000;136:1247–52. http://www.ncbi.nlm.nih.gov/pubmed/11030771.
31. Schiller S, Seebode C, Hennies HC, Giehl K, Emmert S. Palmoplantar keratoderma (PPK): acquired and genetic causes of a not so rare disease. J Dtsch Dermatol Ges. 2014;12:781–8. https://doi.org/10.1111/ddg.12418.
32. Sakiyama T, Kubo A. Hereditary palmoplantar keratoderma "clinical and genetic differential diagnosis.". J Dermatol. 2016;43:264–74. http://www.ncbi.nlm.nih.gov/pubmed/26945534.
33. Richard G, Smith LE, Bailey RA, Itin P, Hohl D, Epstein EH, et al. Mutations in the human connexin gene GJB3 cause erythrokeratodermia variabilis. Nat Genet. 1998;20:366–9. http://www.nature.com/articles/ng1298_366.
34. Macari F, Landau M, Cousin P, Mevorah B, Brenner S, Panizzon R, et al. Mutation in the gene for connexin 30.3 in a family with erythrokeratodermia variabilis. Am J Hum Genet. 2000; 67:1296–301. https://linkinghub.elsevier.com/retrieve/pii/S0002929707629577.
35. Boyden LM, Craiglow BG, Zhou J, Hu R, Loring EC, Morel KD, et al. Dominant de novo mutations in GJA1 cause erythrokeratodermia variabilis et progressiva, without features of oculodentodigital dysplasia. J Investig Dermatol. 2015;135:1540–7. https://linkinghub.elsevier.com/retrieve/pii/S0022202X15372833.
36. Kaliannan K, Hamarneh SR, Economopoulos KP, Nasrin Alam S, Moaven O, Patel P, et al. Intestinal alkaline phosphatase prevents metabolic syndrome in mice. Proc Natl Acad Sci USA. 2013;110:7003–8. https://doi.org/10.1073/pnas.1220180110.
37. Redies C, Hertel N, Hübner CA. Cadherins and neuropsychiatric disorders. Brain Res. 2012;1470:130–44. https://linkinghub.elsevier.com/retrieve/pii/S0006899312010736.
38. Gloushankova NA. Changes in regulation of cell-cell adhesion during tumor transformation. Biochemistry. 2008;73:742–50. http://www.ncbi.nlm.nih.gov/pubmed/18707582.
39. El-Amraoui A, Petit C. Cadherins as targets for genetic diseases. Cold Spring Harb Perspect Biol. 2010;2:a003095. https://doi.org/10.1101/cshperspect.a003095.
40. Jamora C, Fuchs E. Intercellular adhesion, signalling and the cytoskeleton. Nat Cell Biol. 2002;4:E101–8. http://www.nature.com/articles/ncb0402-e101.
41. Fujimori T, Takeichi M. Disruption of epithelial cell-cell adhesion by exogenous expression of a mutated nonfunctional N-cadherin. Mol Biol Cell. 1993;4:37–47. http://www.ncbi.nlm.nih.gov/pubmed/8443408.
42. Pontén FK, Schwenk JM, Asplund A, Edqvist PHD. The Human Protein Atlas as a proteomic resource for biomarker discovery. J Intern Med. 2011;270:428–46.
43. Yin L, Coelho SG, Ebsen D, Smuda C, Mahns A, Miller SA, et al. Epidermal gene expression and ethnic pigmentation variations among individuals of Asian, European and African ancestry. Exp Dermatol. 2014;23:731–5. https://doi.org/10.1111/exd.12518.
44. Del Bino S, Duval C, Bernerd F. Clinical and biological characterization of skin pigmentation diversity and its consequences on UV impact. Int J Mol Sci. 2018;19:2668. https://doi.org/10.3390/ijms19092668